定治具の3D-CAD形状データを有限要素解析ソフトAbaqus（ver. 6.13, SIMULIA）に読み込み実行した．これら脊椎ケージと固定治具を，10節点四面体要素を用いてそれぞれ離散化した（図２－(a) および (b)）．

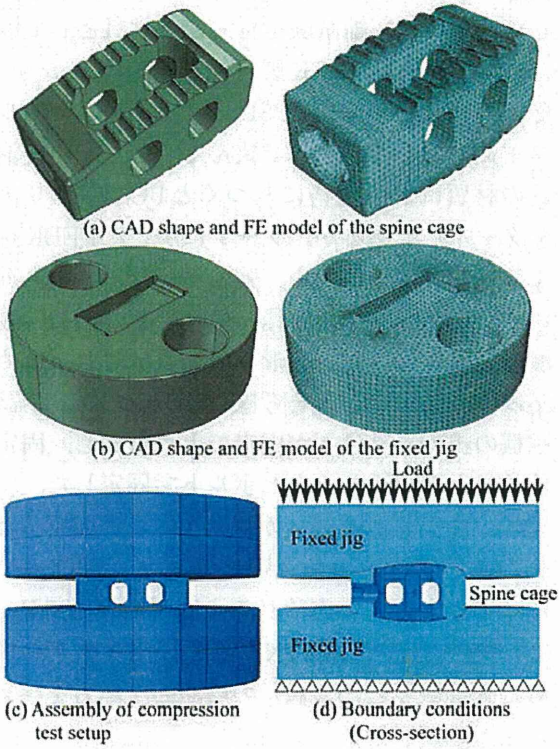

図２．Finite element model of the compression test set up and boundary conditions.

解析対象の材料特性として，ケージおよび治具はともに等方線形弾性体と仮定した．脊椎ケージの材料特性は，PEEKを用いた静的力学試験の結果を参考にヤング率3368MPa，ポアソン比0.4を与えた．治具の材料特性は，PPSUの物性値[6]を参考にヤング率2350MPa，ポアソン比0.4を与えた．

圧縮試験の境界条件は，図２－(d) に示す下方治具の下面を完全固定し，上方治具の上面に実験と同条件の圧縮力を負荷した．脊椎ケージと固定治具のアセンブリにおいて，ケージと治具が接する領域を接触表面とし，接触相互作用特性として摩擦係数0.2の接触条件を設定した．

３．赤外線サーモグラフィ応力測定

得られた応力解析結果の妥当性を評価するために，温度と応力の比例関係を表す熱弾性論に基づき，赤外線サーモグラフィで計測したサンプル表面の温度分布から求めた応力測定結果と，解析によるケージ表面の応力分布結果との比較検討を行った．ケージ表面の温度計測は，高性能赤外線カメラ（CEDIP社製，Silver）を用いた．固体である対象物体に，引張応力を作用させると応力変動に比例した温度が降下し，逆に圧縮応力を作用させれば温度が上昇する熱弾性現象が起きる．サンプル表面の温度変化ΔTは等方均質な線形弾性材料においては次式に示す通り主応力の総和の変化量$\Delta\sigma$（$\Delta\sigma=\Delta\sigma_1+\Delta\sigma_2+\Delta\sigma_3$）に比例する[3]．

$$\Delta T = -K \cdot T \cdot \Delta\sigma \quad \cdots\cdots (1)$$

ここでσ_1は最大主応力，σ_2は中間主応力，σ_3は最小主応力，Tは絶対温度，Kは熱弾性係数である．熱弾性係数は，定圧比熱C_p，線膨張係数αおよび密度ρを用いて次式で与えられる．

$$K = \frac{\alpha}{\rho \cdot C_p} \quad \cdots\cdots (2)$$

熱弾性現象に基づく脊椎ケージの応力測定において，PEEKの熱弾性係数は3.00×10^{-11} Pa^{-1}とした．計測時には対象物表面の放射率を均一にするために，つや消し黒色塗料をケージおよび固定治具表面に塗布した．

結　　果

解析により得られた最大圧縮負荷時における脊椎ケージ表面の相当応力分布を図３に示す．設計における一般的な応力評価では相当応力を用いることが多いことから，ここでも相当応力の結果を示した．図中の（b）はケージの平面図（上面に相当），(c) は左側面図，(d) は正面図である．正面図，平面図，左側面図の定義とその並びは第三角法を参考とした．正面図はケージ形状に対する情報量が最も多い波状突起形状と二つ孔が認められる面を選択した．また，正面図において孔の開いていない右側面側を前方，孔（貫通孔）の開いている左側面図側を後

方とする．脊椎ケージ平面図における波状突起部分，左側面図における貫通孔の孔縁のザグリ部およびその上部に応力の集中が見られた．

赤外線サーモグラフィ応力測定結果との比較を行うために，脊椎ケージの主応力の総和の分布を調べた．温度分布から求められた脊椎ケージ表面の主応力の総和の分布と，解析によって求められた主応力の総和の分布図を図４および図５に示す．図４はケージの正面図，図５は左側面図である．正面図において，赤外線サーモグラフィ応力計測では貫通孔（二つ孔）内側に圧縮が見られ（図中の白抜き矢印），後方に引張が見られた（図中の黒塗り矢印）．解析で得られた主応力和でもケージ貫通孔内側で圧縮，後方に引張が見られた．また，左側面図において，赤外線サーモグラフィ応力計測では，貫通孔の上下に引張，左右（孔縁のザグリ部）に圧縮が見られた．高い圧縮が見られた貫通孔左右のザグリ部では－415.03MPaであった．解析による左側面図の主応力和も，孔の上下に引張が見られ，孔の左右ザグリ部では－325.45 MPaであった．正面図，および左側面図ともに上の固定治具表面に線状の高い引張が見られた．

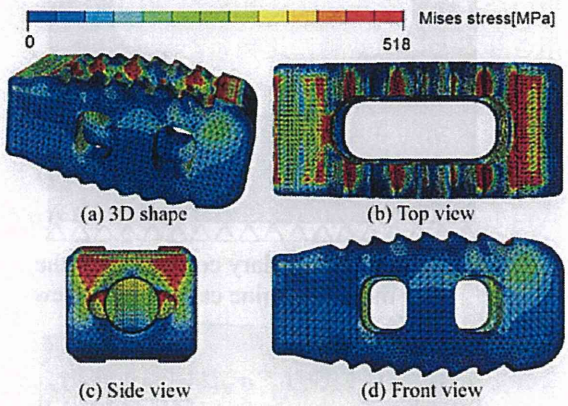

図３．von Mises stress distribution of the spine cage.

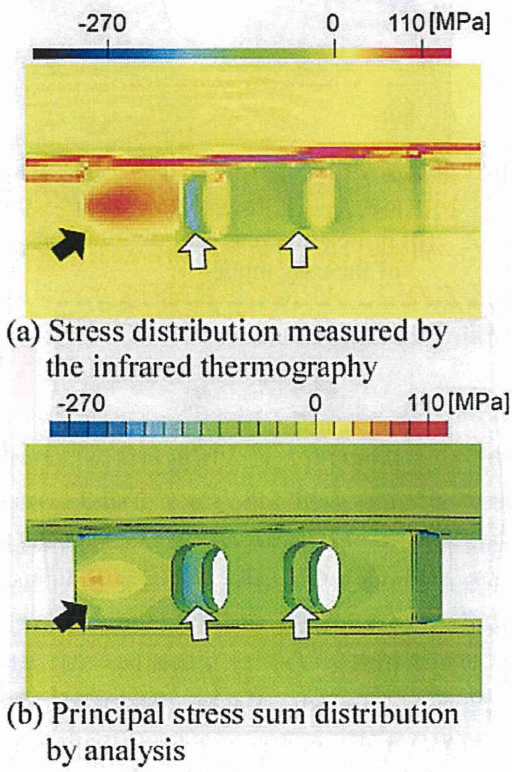

図４．Stress distribution measured by the infrared thermography and principal stress sum distribution over the spine cage (Front view).

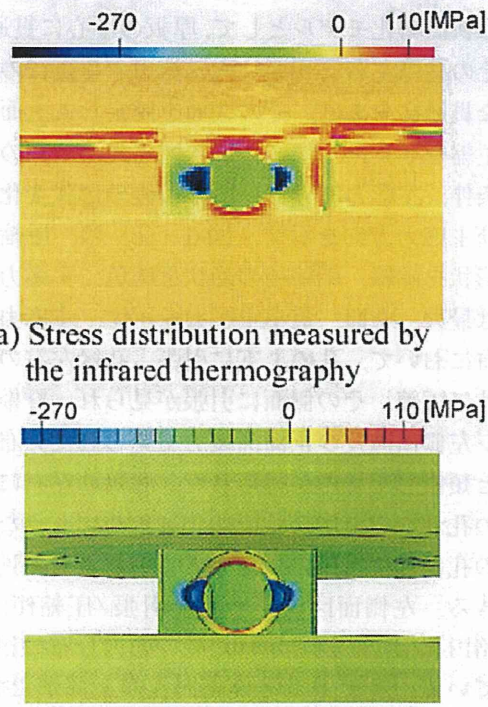

図５．Stress distribution measured by the infrared thermography and principal stress sum distribution over the spine cage (Side view).

考　　察

赤外線サーモグラフィによる応力計測では，正面図において貫通孔内側，および左側面図において孔の左右（孔縁のザグリ部）に圧縮が見られた．解析結果においてケージ貫通孔内側での主応力の総和でも圧縮が見られ，赤外線サーモグラフィによる温度分布測定から推察される応力と，圧縮部位が一致した．また，正面図における後方部位，および左側面図における貫通孔の上下に引張応力が発生していた．赤外線サーモグラフィによる主応力和分布と有限要素解析による主応力和分布とを比較した結果，ケージ表面の引張・圧縮部位が類似していた．この比較から，解析により得られたケージ表面の主応力和の分布は妥当なものと判断できる．

左側面図の貫通孔周囲の主応力和分布，および正面図におけるケージ後方に引張が見られた理由を考察するために，正面図後方1/4の形状簡略化モデルを用いてその応力分布を調べた．形状簡略化モデルとして，厚板の中心に貫通孔，その孔縁左右にザグリ穴に相当する直径の小さな貫通孔をあけ，その底面を固定して上面から圧縮を与えた．図６に形状簡略化モデルの境界条件，主応力和分布，圧縮前後の形状変化および主応力方向を示す．図６－(c) は，圧縮前の形状を破線，圧縮後の形状を灰色，主応力方向は最大，中間，最小主応力を示す．主応力和分布において，孔の上下に引張，孔縁左右の小径孔に圧縮，その側面に引張が見られ，脊椎ケージ左側面図及び正面図後方で見られた分布傾向と類似したものが得られた．孔縁の左右に小径の孔が空いた本形状簡略化モデルのような三連の孔は等価楕円の概念より楕円孔として近似できる．左側面図に見られた引張/圧縮傾向は，楕円孔板に圧縮をかけた時の応力分布に相当している．モデルは等価楕円孔の上部がたわみ，横方向に膨らむ形で変形した．主応力は横方向に膨らんだ位置に引張がわずかに見られた．したがって，ケージの正面図後方に見られた引張は，左側面に空いた等価楕円孔の形状変化により発生したと考えられる．ケージ表面に見られ

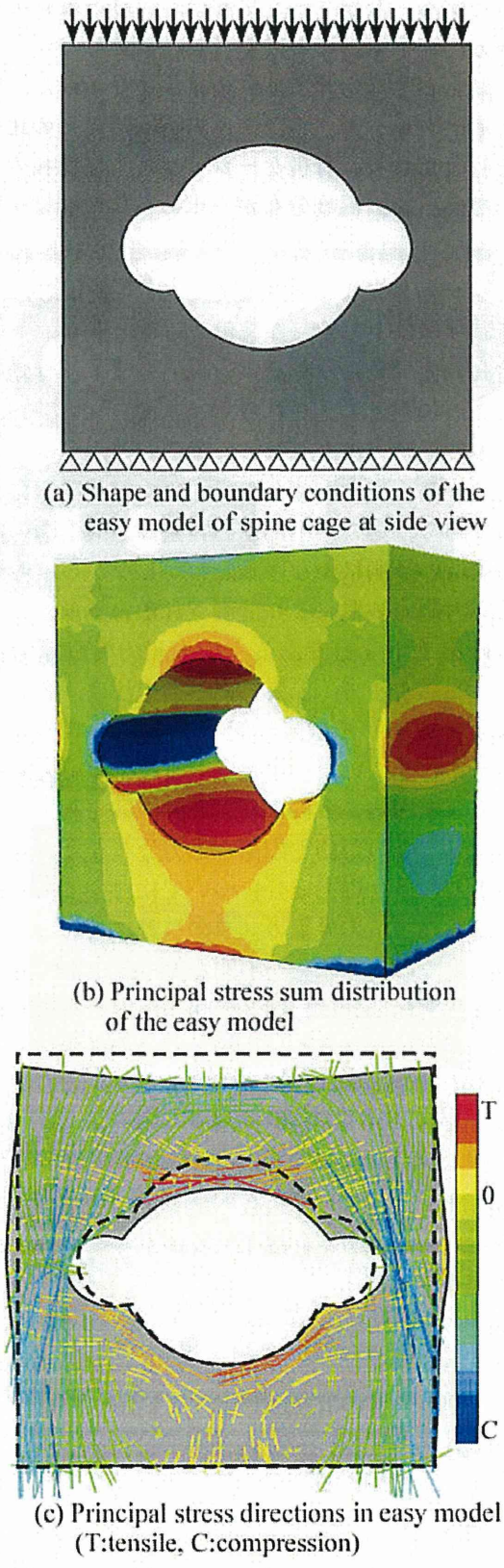

(a) Shape and boundary conditions of the easy model of spine cage at side view

(b) Principal stress sum distribution of the easy model

(c) Principal stress directions in easy model (T:tensile, C:compression)

図６．Stress distribution of the easy model of spine cage at side view.

た特徴的な引張/圧縮応力分布は形状簡略化モデルの結果から妥当なものといえる．

図4および図5の赤外線サーモグラフィによる主応力和分布において上の固定治具の表面で高い引張応力が認められた．赤外線測定では同じ位置の画素の温度を測定しており，エッジ部が動くと温度が変化していると測定されるエッジ効果による誤差が起こる[1]．使用した万能試験機は上の治具が稼働することから，上の治具表面で見られた高い引張応力はエッジ効果による誤差と考えられる．

赤外線サーモグラフィによる応力測定は，局部的に高い応力が加わる応力集中部位特定に有用である．応力集中部位の特定は，構造物の破損箇所の予測につながる．しかしながら，赤外線応力測定装置により計測される力学量は，応力の第1不変量である主応力和の変動量である．したがって，赤外線応力測定法は，各応力成分を分離して直接計測できない[1]．3D-CADデータに基づいた有限要素解析による応力分布と整合を図ることにより，赤外線応力測定装置では見えない裏側や内部の応力分布などが推定表示でき，各応力成分について検討することが可能となる．赤外線カメラの視野に入らないため測定では応力状態が不明なケージ上面と底面の波状突起部分は，図3の相当応力分布では高い応力が確認された．このように赤外線応力測定と有限要素解析とを組み合わせた応力評価は，設計において重要な指標となる相当応力なども正確に評価できる可能性がある．これらの応力測定によって得られた結果は，破損が予測される応力集中を低減する脊椎ケージ形状の提案につながる．

結　　言

脊椎ケージの3D-CADデータに基づいた圧縮試験の有限要素シミュレーションを行い，ケージ表面および内部の応力分布を評価することができた．脊椎ケージ表面の主応力和分布は，赤外線サーモグラフィによるケージ表面の温度分布測定から推察される応力分布と圧縮・引張箇所が一致した．計測と解析による応力分布の整合性が取れれば，赤外線カメラ視野外のケージと治具との接触領域や内部の応力に対し，有限要素解析を通して評価できる可能性が示唆された．

＜謝　　辞＞

本研究の一部は，厚生労働科学研究費補助金の助成を受けたものである．

赤外線カメラによる応力測定では，JFEテクノリサーチ株式会社のご協力のもとで実施された．

文　　献

1）坂上隆英：赤外線サーモグラフィによる非破壊検査（2）赤外線サーモグラフィによる熱弾性応力測定．溶接学会誌 72：511-515，2003.
2）永村和真，中西義孝 他：椎体間スペーサー開発における力学試験とFEM解析の比較．臨床バイオメカニクス 34：33-40，2013.
3）西名慶晃，今西大輔 他：高精度赤外線サーモグラフィを活用した各種測定技術（温度・応力・疲労・亀裂）とその応用．JFE技報 27：9-14，2011.
4）兵藤行志，野中勝信 他：バイオメカニカル光イメージング．産総研TODAY 9：9，2009.
5）松下富春，小久保正 他：チタン多孔体を用いた脊椎固定術用椎間スペーサーの開発．生命健康科学研究所紀要：20-29，2009.
6）PPSU樹脂，Material Data Sheet 2012年09月版，エンズィンガージャパン株式会社．

ARTICLE IN PRESS

CARBON XXX (2014) XXX–XXX

Available at www.sciencedirect.com

ScienceDirect

journal homepage: www.elsevier.com/locate/carbon

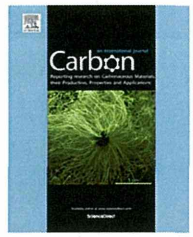

Radical scavenging reaction kinetics with multiwalled carbon nanotubes

Shuji Tsuruoka [a,*], *Hidetoshi Matsumoto* [b], *Kenichi Koyama* [a], *Eiji Akiba* [c], *Takashi Yanagisawa* [d], *Flemming R. Cassee* [e,f], *Naoto Saito* [g], *Yuki Usui* [a], *Shinsuke Kobayashi* [g], *Dale W. Porter* [h], *Vincent Castranova* [i], *Morinobu Endo* [j]

[a] *Aquatic Innovation Center, Shinshu University, 4-17-1 Wakasato, Nagano 380-8553, Japan*
[b] *Department of Organic and Polymeric Materials, Tokyo Institute of Technology, 2-12-1 Ookayama, Meguro-ku, Tokyo 152-8552, Japan*
[c] *Kuraray Living Co., Ltd., 8-1 Kadota-cho, Osaka 530-8611, Japan*
[d] *GSI Creos Corporation, 1-12, Minami-Watada-cho, Kawasaki, Kanagawa 210-0855, Japan*
[e] *National Institute for Public Health & Environment, Antonie van Leeuwenhoeklaan 9, 3721 Bilthoven, MA, The Netherlands*
[f] *Institute for Risk Assessment Sciences, Utrecht University, Yalelaan 104, 3584 CM Utrecht, The Netherlands*
[g] *Department of Applied Physical Therapy, Shinshu University, School of Health Sciences, 3-1-1 Asahi, Matsumoto, Nagano, Japan*
[h] *National Institute for Occupational Safety and Health, Pathology & Physiology Research Branch, 1095 Willowdale Rd. (M/S2015), 26505-2888 Morgantown, WV, USA*
[i] *Department of Basic Pharmaceutical Sciences, West Virginia University, School of Pharmacy, 26506 Morgantown, WV, USA*
[j] *Institute of Carbon Science and Technology, Shinshu University, Nagano 380-8553, Japan*

ARTICLE INFO

Article history:
Received 30 May 2014
Accepted 3 October 2014
Available online xxxx

ABSTRACT

Progress in the development of carbon nanotubes (CNTs) has stimulated great interest among industries providing new applications. Meanwhile, toxicological evaluations on nanomaterials are advancing leading to a predictive exposure limit for CNTs, which implies the possibility of designing safer CNTs. To pursue safety by design, the redox potential in reactions with CNTs has been contemplated recently. However, the chemical reactivity of CNTs has not been explored kinetically, so that there is no scheme to express a redox reaction with CNTs, though it has been investigated and reported. In addition, the reactivity of CNTs is discussed with regard to impurities that consist of transition metals in CNTs, which obfuscates the contribution of CNTs to the reaction. The present work aimed at modeling CNT scavenging in aqueous solution using a kinetic approach and a simple first-order reaction scheme. The results show that CNTs follow the redox reaction assumption in a simple chemical system. As a result, the reaction with multiwalled CNTs is semi-quantitatively denoted as redox potential, which suggests that their biological reactions may also be evaluated using a redox potential scheme.

1. Introduction

Carbon nanotubes (CNTs) may be useful for various medical, commercial, and industrial applications, and designing their structures has recently become an important issue in order to obtain tailor-made performances [1]. At present, their diameter and length are only rudimentarily controllable, while in the laboratory diameter-controlled double-walled

* *Corresponding author.*
E-mail address: s_tsuruoka@shinshu-u.ac.jp (S. Tsuruoka).
http://dx.doi.org/10.1016/j.carbon.2014.10.009
0008-6223/

Please cite this article in press as: Tsuruoka S et al. Radical scavenging reaction kinetics with multiwalled carbon nanotubes. Carbon (2014), http://dx.doi.org/10.1016/j.carbon.2014.10.009

CNTs (DWCNTs) were synthesized [2,3]. The inner space of CNTs is utilized to deliver particular performances with various particles [4,5]. Industrially, atypical multiwalled CNTs (MWCNTs) are applied and commercialized [6–11]. Thus, modifications of CNT structures will become an important issue to synthesize and obtain appropriate functionalities and safety in use. Among the challenges with CNTs, particularly MWCNTs, a new and crucial goal will be to design safe CNT structures, while toxicological evaluations on CNTs are advancing leading to a predictive exposure limit for MWCNTs [12]. This groundbreaking challenge requires the identification of a key mechanism that controls toxicological phenomena [13]. The importance of physicochemical properties is often proposed, but the relative importance of specific properties has not been defined explicitly. Two critical points concerning CNT safety evaluations are summarized as the fiber paradigm and bioactivity, for example, the metal impurities of CNTs [14]. The former applies to not only CNTs but also other nanowires and microfibers and refers to the effects of physical contact with cells and tissues. The latter can be described as chemical reactions on the CNT surface and suggests an intrinsic phenomenon related to biological activities. The metal impurity issue has obscured the contribution of CNTs themselves to bioactivity. Thus, it is necessary to develop a model describing a reaction mechanism for CNTs.

Recent investigations suggest that an intrinsic CNT reaction mechanism may be described by a redox reaction system, because iron is not available on the CNT surface when Fe(III) oxides were formed [15,16]. These impurity effects and their removal are copiously discussed relating to their bioactivities [17–22]. A voltammetric method was used to compare the redox potential of SWCNTs to glassy carbons and associated with the redox potential of CNTs [20]. Nevertheless, Y. Liu et al. pointed out that these articles were inconclusive and could not be compared to each other [21]. They discussed that CNTs not only activate the specific molecular signaling associated with the oxidative stress activator protein but also exhibit reactive oxygen species (ROS) scavenging properties. Later, it was reported that, because these metals were capsulated into carbon shells, transition metals were not eluted by an acid wash and were not bioavailable [22].

To various degrees, transition metal impurities are usually oxidative to peroxides, while metal oxides are relatively stable. It is known that Fe(II) or Fe^{2+} ion generates hydroxyl radicals ($OH^{\cdot}$), a form of ROS, in the presence of hydrogen peroxide by the Fenton reaction, and that ROS induce inflammation of tissues. By contrast, Fe(III) oxide (Fe_2O_3) and carbide (FeC) do not generate ROS, because Fe(III) cannot be an electron donor except upon treatment with a strong reduction agent. As Fe(II) is supplied not only externally as metal impurities but also internally in a living body and essentially catalyzes peroxide-generating hydroxyl radicals, reduction reactions are required to eliminate the radicals. A question is whether the redox potential of CNTs is predictive of ROS generation [13], as CNTs inevitably have chemical reaction sites, for instance, dangling bonds. As of today, it has not been determined if CNT surfaces behave as electron donors or acceptors. If these reaction sites donate electrons to radicals, CNTs become ROS scavengers in an aqueous system.

The present work objectively investigated the chemical reactivity and redox potential of MWCNTs pseudo-quantitatively using its known scavenging ability for hydroxyl radicals. As the chemical reactivity has not been kinetically explored extensively, we hypothesized a simple first-order chemical reaction system for MWCNTs, hydrogen peroxide, and hydroxyl radicals, and designed an experimental method to verify the assumption. To embody it, chemical reactions with these components were investigated to eliminate unnecessary disturbances as much as possible. The present studies suggest that the experimental results agree with the assumption, which validates the study of redox potential to evaluate the chemical reactivity of CNTs.

2. Experimental

2.1. MWCNTs

Two kinds of MWCNTs were used in the present work: cup-stack MWCNTs (CS-MWCNTs) prepared by GSI Creos Corporation (Tokyo, Japan) and Nanocyl NC-7000 MWCNTs obtained from Nanocyl. The average diameter and length of CS-MWCNTs were 80 nm and 5 μm, respectively. In addition, the average diameter and length of Nanocyl NC-7000 were 9.5 nm and 1.5 μm, respectively. The former was provided in order to evaluate the influence on the scavenging performance of the chemical components. As CS-MWCNTs have many graphene edges on their surface as shown in Fig. 1, they might be relatively reactive chemically. CS-MWCNTs were characterized in a previous article [26]. The latter was used to measure the intrinsic radical scavenging rate of MWCNTs using a typical MWCNT produced by the catalytic chemical vapor deposition method. To reduce the surfactant amount to a minimal concentration against MWCNTs and obtain their

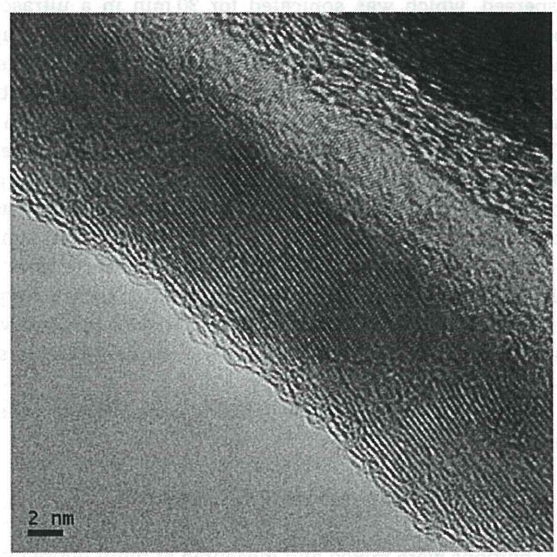

Fig. 1 – An electron microscopy picture of a CS-MWCNT. Graphene layers are stacked and are not parallel to the fiber axis. There are edges of graphene sheets on the surface.

Please cite this article in press as: Tsuruoka S et al. Radical scavenging reaction kinetics with multiwalled carbon nanotubes. Carbon (2014), http://dx.doi.org/10.1016/j.carbon.2014.10.009

good dispersion in water, a specially prepared CNTEC® produced by Kuraray Living Co., Ltd., (Tokyo, Japan) was used as described in Section 2.2.

2.2. Preparation of mixtures and ESR-DMPO method

The measuring mixture consisted of MWCNTs, hydrogen peroxide, ferrous chloride, and 5,5-dimethyl-1-pyrroline-1-oxide (DMPO). Hydrogen peroxide (hydrogen peroxide 30.0–35.5 mass%, Wako Pure Chemical Industries, Ltd., Osaka, Japan) was diluted to 0.1 M with ultrapure water. The 0.1 M solution was diluted to 1 mM with ultrapure water before use. Ferrous chloride (iron (II) chloride tetrahydrate, Wako Pure Chemical Industries, Ltd., Osaka, Japan) was dissolved in ultrapure water to 15.7 mM. This solution was also diluted 100 times before use. Frozen DMPO (Dojindo Laboratories, Kumamoto, Japan) was thawed at room temperature and diluted to 100 mM with ultrapure water. The DMPO solution was prepared each time and disposed within 24 h after preparation. The surfactant for CS-MWCNTs was sodium dodecyl benzensulfonate (SDBS) (Kanto Chemical Co., Inc., Tokyo, Japan) and was diluted to 45.9 mM with ultrapure water.

CNTEC® was made of polyester fibers coated with 12 wt% Nanocyl NC-7000 in dry condition. The weight ratio of the concentration of the surfactant to MWCNTs of CNTEC®, which was specially prepared, was fixed at 26.2:100 in dry condition. In 50 g of ultrapure water, 0.1 g CNTEC fibers were dispersed, which was sonicated for 30 min in a ultrasonic bath. The mixture was filtered with a Whatman filter paper (Whatman 42 with pore size at 2.5 μm) to remove polyester fibers and large agglomerates of MWCNTs. This solution was named as Solution A, which included 0.13 wt% of MWCNTs after drying the solution. Solution A was filtered with a Whatman filter paper (GF/F with pore size 0.7 μm) and then a Milipore filter (MF-Milipore GSWP 09000 m with pore size at 0.22 μm). This solution, named Solution B, included 0.036 wt% of MWCNTs. The procedure gave an advantage to balancing the surfactant interference despite alterations in MWCNT concentration. These solutions were used instead of CS-MWCNTs that were dispersed in the surfactant solution.

In all measurements, the peroxide concentration was in excess.

2.3. Electron spin resonance measurement

All solutions were mixed and measured at room temperature with electron spin resonance (ESR) (JES-FA100, JEOL). The ESR settings were as follows: frequency 9415.404 MHz, power 0.998 mW, field center 335 mT, sweep time 2 min, width ± 5 mT, and modulation frequency 100 kHz. All measurements were conducted within 5 min after mixing all of the solutions. The details were reported in a previous article [26].

ESR spectra were normalized using Mixture B in Table 1 with 0.1 ml CNT solution for all of the CS-MWCNT measurements. With Nanocyl NC-7000, Mixture A in Table 1 without surfactant was used. The ESR measurement results were obtained as relative values to a reference. In the present work, the radical concentration in a reference solution or specified MWCNT mixture was described using the normalized form:

$$\text{Scavenging ratio} = [\text{ESR signal of a sample/ESR signal of a reference}] = [\text{radical concentration of a sample /radical concentration of a reference}]$$

As the ratio is 1 at MWCNT = 0, radical concentration with a change of CNT concentration was expressed as radical concentration ratio to the reference. On the other hand, the radical scavenging rate is described as:

$$\text{Scavenging rate} = \{1 - (\text{Scavenging ratio})\}$$

ESR spectra were normalized using Mixture B in Table 1 with 0.1 ml CNT solution for all of the CS-MWCNT measurements. With Nanocyl NC-7000, Mixture A in Table 1 without surfactant was used. Thus, the scavenging ratio and rate represent the normalized hydroxyl radical concentration relative to the reference and the normalized hydroxyl radical concentration amount scavenged in a solution, respectively. All of the samples were measured at least five times and arithmetically averaged except the lowest and highest values. In the present work, a buffer to control solution pH was not added because the buffer apparently affects the reaction and the reactive components were in the aqueous solution. pH measurement was not conducted during ESR-DMPO measurement because it cannot be physically measured during the ESR spectrum measurements.

3. Results and discussion

3.1. Reaction kinetics hypothesized

According to recent findings, MWCNTs scavenge ROS [23–26]. All of these reports hinted that the reaction occurs at dangling bonds on CNT surfaces and MWCNTs supposedly act as electron donors or, at least, charge is transferred from those dangling bonds to radicals. Petersen et al. reported that SWCNTs also scavenge hydroxyl radicals by electron transfer [27]. Peng et al. found that MWCNTs attached with cadmium sulfide (CdS) were electron acceptors and catalyzed the conversion of water to hydrogen (and inevitably oxygen) in a photoreaction as a simulated photosynthetic reaction, where radical formation and degeneration were implicitly included [28]. This indicates that MWCNTs can be both electron acceptors and donators in redox reactions depending on their relative chemical potentials. If the redox potential is hypothesized for MWCNTs, they may decrease oxidant-induced inflammation of tissues, though the actual condition

Please cite this article in press as: Tsuruoka S et al. Radical scavenging reaction kinetics with multiwalled carbon nanotubes. Carbon (2014), http://dx.doi.org/10.1016/j.carbon.2014.10.009

Table 1 – Solution mixture components for CS-MWCNTs.

Amount of solutions taken (ml)							
Solutions	$FeCl_2$	CNTs in surfactant	DMPO	Surfactant	H_2O_2	Ultrapure water	Total volume
Mixture A	0.4	None	0.4	0.4–0.8	0.4	Balance	2.0
Mixture B	0.4	0–0.4	0.4	Balance	0.4	0.4	2.0

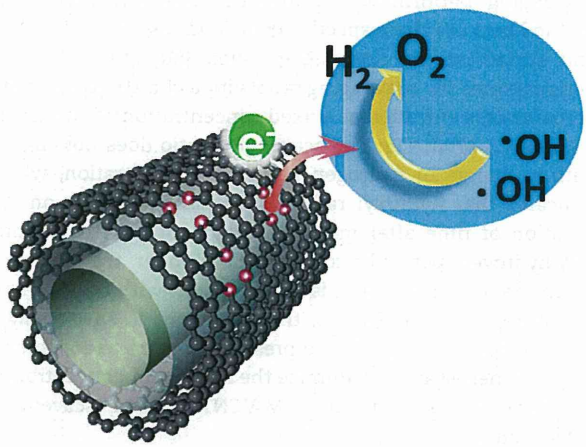

Fig. 2 – A schematic diagram to illustrate hypothesized reaction kinetics of hydroxyl radicals at a reaction site of MWCNTs. For easy visualization of the assumed concept, it is illustrated as if the reaction takes place at a dangling bond. Reaction sites donate electrons to hydroxyl radicals and result in hydrogen and oxygen as denoted in Eq. (6). (A color version of this figure can be viewed online.)

surrounding MWCNTs is complicated. One would be able to stoichiometrically predict oxidant stress once the redox potential of MWCNTs is determined in a reaction system. To conduct and specify CNT behavior in aqueous solution, it is necessary to model it using a simple first-order reaction profile for CNTs as the first step.

We hypothesize the following chemical reaction equations with MWCNTs and hydrogen peroxide (Fig. 2). First, in the light of the fact that a description of the Fenton reaction has not been agreed upon completely, a simple system consisting of hydrogen peroxide and Fe(II) can be written to characterize the present experimental system specifically as follows [29,30]:

$$Fe^{2+} + H_2O_2 \rightarrow Fe^{3+} + HO^- + HO^{\cdot} \quad (1)$$

$$Fe^{3+} + H_2O_2 \rightarrow Fe^{2+} + H^+ + HOO^{\cdot} \quad (2)$$

$$Fe^{3+} + HOO^{\cdot} \rightarrow Fe^{2+} + H^+ + O_2 \quad (3)$$

These equations can be summarized as follows:

$$3H_2O_2 \rightarrow 2H_2O + O_2 + 2HO^{\cdot} \quad (4)$$

According to previous reports [12,20,22–25], it is agreed that CNTs scavenge hydroxyl radicals in an aqueous solution with hydrogen peroxide experimentally. The assumed reaction sites on the CNT surface including dangling bonds are denoted as Dn that acts as if they were single molecules. As long as Eq. (4) is true, a necessary condition to satisfy it with radical scavenging must become an equation as follows:

$$2Dn + 2HO^{\cdot} \rightarrow 2Dn^+ + H_2 + O_2 \quad (5)$$

Accordingly, Eqs. (4) and (5) give the following equation:

$$3H_2O_2 + 2Dn \rightarrow 2Dn^+ + 2H_2O + H_2 + 2O_2 \quad (6)$$

Eq. (5) indicates that the reaction sites donate electrons to hydroxyl radicals finitely. This agrees with the assumption of H+ or OH radical generation by electron acceptance on CNTs by Peng et al. [28] In Eq. (6), the reaction rate constant should become "1" if the concentration of Dn is large enough and dominates compared to that of H_2O_2 from Eqs. (S5) to (S6) in the Supplemental. This suggests that this experimental condition must be avoided. Furthermore, the equations predict that the CNT amount, or mole equivalent of the number of reaction sites, is necessarily smaller than that of hydrogen peroxide. Thus, while the mole equivalent of CNTs or reaction sites has not been determined, a concentration ratio of hydrogen peroxide to CNTs should be sought in an experiment.

Eq. (5) requires one to measure the concentrations of hydrogen and oxygen in a scavenging reaction in order to verify the Fenton reactions. However, it is experimentally impossible to measure these concentrations in situ because of the measuring system of the ESR equipment and its measuring cell structure. Fortunately, Eq. (5) is a fictitious reaction to deduce Eq. (6) so that Eq. (5) is regarded as an intermediate reaction. Although the Fenton reaction gives many routes of reaction steps, it can be simplified in such a manner.

3.2. *Influences of chemicals in a reaction system*

Before conducting chemical tests to investigate whether Eq. (6) is appropriate to describe the present chemical reaction, it is necessary to investigate influences by chemicals in an ROS measurement. This has not been pursued previously, because the present approach with chemical kinetics had not been proposed nor systematically explored. In addition, it was reported that chemicals in similar systems significantly affect ESR-DMPO measurement [31]. We conducted a series of tests using CS-MWCNTs (Fig. 1), because they have many edges of graphene that are relatively reactive in comparison with highly crystallized CNTs [26]. Fig. 3a shows that the radical scavenging rate varies with a concentration change of the surfactant without CS-MWCNTs, where Mixture A in Table 1 was used. A reference solution was at 0 mM of the surfactant of Mixture A in Table 1. The results show that hydroxyl radicals are scavenged proportional to a surfactant concentration. Fig. 3a apparently indicates that the surfactant scavenges radicals. Fig. 3b shows the radical scavenging rate

Please cite this article in press as: Tsuruoka S et al. Radical scavenging reaction kinetics with multiwalled carbon nanotubes. Carbon (2014), http://dx.doi.org/10.1016/j.carbon.2014.10.009

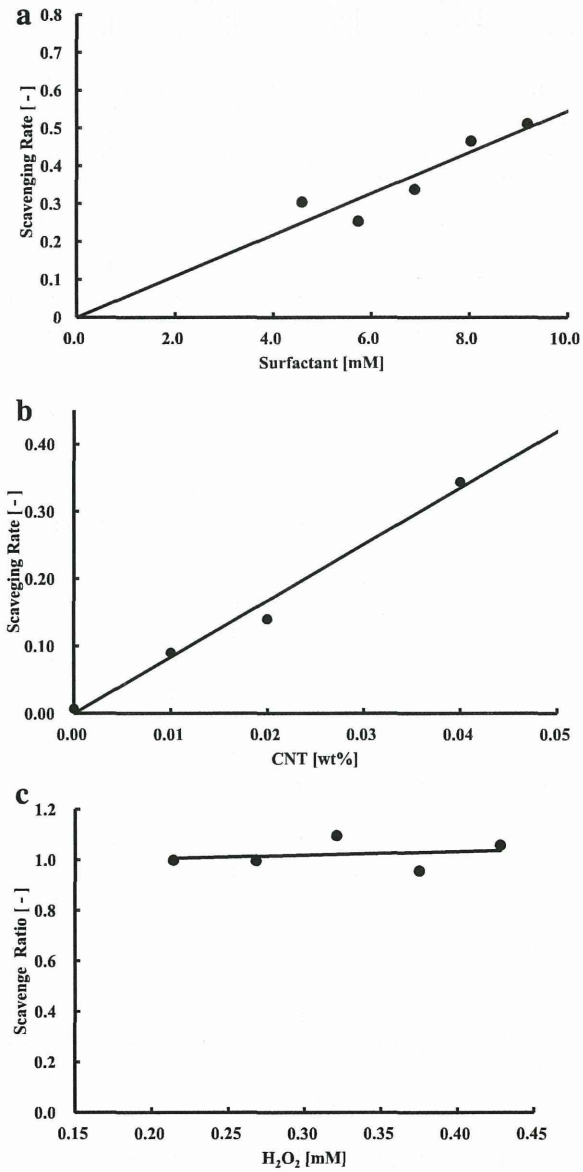

Fig. 3 – Influences of chemical components in the scavenging reaction system. Vertical axis shows the scavenging rate of hydroxyl radicals that were generated by the Fenton reaction with hydrogen peroxide. (a) Influence of surfactant without CS-MWCNTs. The scavenging rate is proportional to surfactant concentration. (b) A scavenging rate change with a change of CS-MWCNT concentration at a fixed surfactant concentration of 0.918 mM. Scavenging rate proportionally corresponds to the MWCNT concentration change. (c) The scavenging ratio with a change of hydrogen peroxide concentration in fixed concentrations of $FeCl_2$ and surfactant in Mixture B without CS-MWCNTs in Table 1. It is apparent that the radical concentration is constant at the measuring time in the solution.

with a concentration change of MWCNTs in a fixed concentration of surfactant at 0.918 mM in a solution, where Mixture B was used in Table 1. Likewise, the reference solution was at 0 wt% of MWCNTs of Mixture B in Table 1. As the scavenging rate of hydroxyl radicals proportionally corresponds to the surfactant concentration according to Fig. 3a, Fig. 3b indicates that the scavenging rate is proportional to the concentration change of CS-MWCNTs at a fixed surfactant concentration, where the surfactant contribution is relatively low. This suggests that the ESR-DMPO method can measure radical concentration changes corresponding to a CS-MWCNT concentration change. However, an intrinsic CS-MWCNT scavenging performance cannot be measured using this method because the respective contributions of CS-MWCNTs and surfactant are not distinguished individually. Fig. 3c demonstrates the scavenging ratio with a change of hydrogen peroxide concentration at a fixed concentration of surfactant without CS-MWCNTs. The scavenging ratio does not change with a change in hydrogen peroxide concentration, which indicates that hydroxyl radical generation depends on the duration of time after mixing these chemicals rather than the hydrogen peroxide concentration under the proposed experimental condition. It is in agreement with the previous literature [29,30]. Therefore, the surfactant is specifically a major influence factor in the present chemical reaction system. It is necessary to minimize the surfactant concentration to determine the intrinsic MWCNT radical scavenging performance.

In our radical scavenging tests with MWCNTs, pH measurements were omitted. On the one hand, there is physical obstruction in which the DMPO adduct has a very short lifetime and the measuring cell cannot be equipped with a pH cell inside due to physical constraints. It did not allow the measurement of pH in situ. On the other hand, the interaction among the buffer chemicals, MWCNTs, and DMPO is complicated and cannot be predicted. The reaction sites on MWCNTs might react with phosphate and DMPO could attach on the CNT surface [32]. It is noted that the pH of the solution mixture just before ESR measurement was approximately 6.5; this was almost equal to that of ultrapure water used. It is regarded that water stabilized pH due to the very low concentration. It would be optimal to estimate or measure the solution pH during ESR-DMPO spectra measurement.

3.3. *Scavenging performance measurements with the minimal amount of surfactant and intrinsic redox potential of MWCNTs*

As mentioned above, because of the influence of surfactant scavenging, performance measurements were conducted using a minimal amount of surfactant with MWCNTs to determine the intrinsic contribution of MWCNTs to radical scavenging. Fig. 4 shows a change in scavenging rate with a change of MWCNT solution volume, where Solution A or B was added into water. This figure clearly shows that the radical scavenging depends on MWCNT concentration. In this procedure, the surfactant concentration in Solutions A and B was identical. Because these solutions were diluted further with ultrapure water and hydrogen peroxide in the measurement, surfactant concentration was two to three digits lower than that of Mixture A or B, which were prepared using a conventional method with surfactant. As the surfactant amount was proportional to the MWCNT concentration which was

Please cite this article in press as: Tsuruoka S et al. Radical scavenging reaction kinetics with multiwalled carbon nanotubes. Carbon (2014), http://dx.doi.org/10.1016/j.carbon.2014.10.009

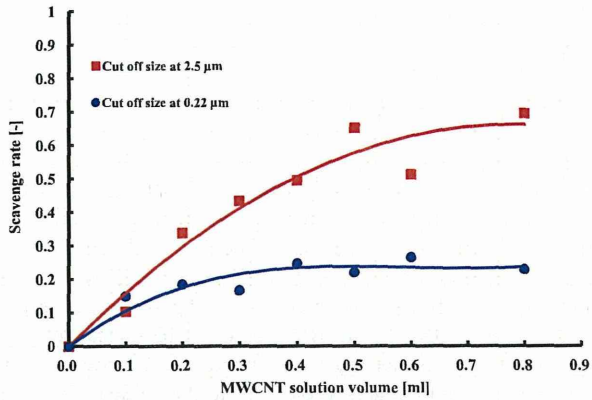

Fig. 4 – Radical scavenging rate with a volume change of MWCNT solutions A and B. Solutions A and B are filtered at 2.5 and 0.22 μm, respectively, to control MWCNT weight concentration. These fitting curves are binominal for Solution A and section three approximations for Solution B, respectively. From these fitting curves, the equilibrium points of Solutions A and B are found to be at 0.78 and 0.38, respectively. (A color version of this figure can be viewed online.)

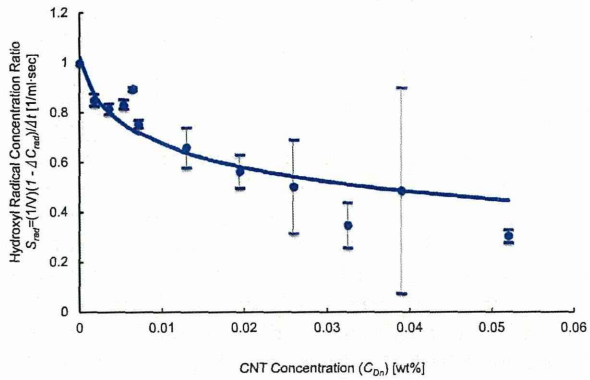

Fig. 5 – A change of hydroxyl radical concentration S_{rad} in the solution with a change of MWCNT weight concentrations C_{Dn}. The solid line is calculated using Eq. (7). Standard deviations of these plots by measurement are indicated with vertical bars. (A color version of this figure can be viewed online.)

low, the influence of the surfactant was believed to be negligible in Solutions A and B according to Fig. 3a. Fig. 4 demonstrates that the maximum of the hydroxyl radical scavenging rate depends on MWCNT concentration and shows their plateau points. This result suggests that the number of reaction sites was significantly different between these solutions.

In comparison with the experimental results discussed in the previous section, the curvature in Fig. 4 is apparently different from that in Fig. 3b. Although it was true that the size distributions of MWCNTs in Solutions A and B were not identical after passing through those filters, the tendency of these curves was alike. The results are consistent with a previous report in which the size difference of particular MWCNTs did not significantly affect the scavenging characteristics though the surface morphological difference did [26]. Another report used MWCNT weight concentration in the horizontal axis instead of volumetric concentration used in Fig. 4. A single smooth line resulted when these results were plotted against each other [31]. From these facts, it is suggested that the scavenging reaction is proportional to the surface area of MWCNTs or the number of reaction sites. Besides, Fig. 4 indicates that the scavenging rate does not increase in a straight line as in Fig. 3a, or the first-order reaction to CNT concentration. Even though peroxide was excessive in quantity, radicals were generated but not so rapidly. Therefore, the scavenging rate exhibits a plateau. It indicates that there is an equilibrium point by an unknown mechanism. However, this is not the target of the present study. Thus, Eq. (5) is an intermediate reaction simply given to derive Eq. (6) with the Fenton reactions.

In Fig. 5, all plots measured with Solutions A and B are summarized together. The solid line is calculated by Eq. (7) as:

$$S_{rad} = -q\ ln|C_{Dn} + s| + q(C_{Dn} + s) + r \tag{7}$$

where S_{rad} and C_{Dn} are the scavenging ratio and the MWCNT concentration in a mixture. Detailed definitions are given in the Supplemental. Note that Eq. (7) is equivalent to Eq. (S8′) in the Supplemental. In Eq. (7), q, r, and s are arbitrary constants and were calculated using the "Solver" function of Microsoft Excel (Microsoft® Excel® for Mac 2011, Version 14.3.9) to be 0.14936, 0.00000, and 0.00105, respectively. Fig. 5 clearly shows that the scavenging reaction ratio or the hydroxyl radical concentration ratio measured agrees with the solid line practically, which indicates that the hypothesis in Eq. (6) is appropriate to denote the reaction system.

Fig. 5 evidently shows that the experimental result agrees with Eq. (7). In Fig. 4, on the one hand, the results are individually plotted based on these prepared MWCNT solutions in order to show CNT concentration dependency. In Fig. 5, on the other hand, all plots are processed together with a change of CNT weight concentration. The former sets forth the radical scavenging reaction depending on the MWCNT surface amount. It is regarded as a technique to detect the reaction rates at very low concentrations of MWCNTs without a change of the other ingredients in the solution. The latter is used to analyze the reaction kinetics. These measurement standard deviations tend to be small at the lower MWCNT concentrations. It is probable that radical scavenging by the surfactant may become significant at higher MWCNT concentrations as the surfactant concentration is proportional to the MWCNT concentration. It is necessary to look for a method to determine the reaction rates of hydroxyl radicals–DMPO and hydroxyl radicals–surfactant to verify the point.

The plateau point is supposed as a pseudo-equilibrium point in this particular reaction system, and may be related to the number of reaction sites of MWCNTs. However, when Eq. (7) is expanded using the Taylor expansion, it is rewritten, if C_{Dn} is large enough, as:

$$S_{rad} = -q\left\{2\left(C_{Dn} + \frac{C_{Dn}^3}{3} + \cdots + \frac{C_{Dn}^{2n+1}}{2n+1} + \cdots\right)\right\} + qC_{Dn} + r$$
$$= -q(C_{D}n) + \cdots + \frac{C_{Dn}^{2n+1}}{2n+1} \tag{7′}$$

Please cite this article in press as: Tsuruoka S et al. Radical scavenging reaction kinetics with multiwalled carbon nanotubes. Carbon (2014), http://dx.doi.org/10.1016/j.carbon.2014.10.009